Extreme Mechanics Letters 48 (2021) 101377

Contents lists available at ScienceDirect

Extreme Mechanics Letters

journal homepage: www.elsevier.com/locate/eml

Ensembles of the leaf trichomes of *Arabidopsis thaliana* selectively vibrate in the frequency range of its primary insect herbivore

Jun Yin [a,b], Han Liu [c], Jiaojiao Jiao [d], Xiangjun Peng [d,e], Barbara G. Pickard [e], Guy M. Genin [e], Tian Jian Lu [a,b,d,*], Shaobao Liu [a,b,*]

[a] State Key Laboratory of Mechanics and Control of Mechanical Structures, Nanjing University of Aeronautics and Astronautics, Nanjing 210016, PR China
[b] MIIT Key Laboratory of Multifunctional Lightweight Materials and Structures, Nanjing University of Aeronautics and Astronautics, Nanjing, 210016, PR China
[c] Collaborative Innovation Center for Chinese Medicine and Respiratory Diseases co-constructed by Henan province & Education Ministry of PR China, Academy of Chinese Medical Sciences, Henan University of Chinese Medicine, Zhengzhou 450016, PR China
[d] State Key Laboratory for Strength and Vibration of Mechanical Structures, School of Aerospace, Xi'an Jiaotong University, Xi'an 710049, PR China
[e] National Science Foundation Science and Technology Center for Engineering Mechanobiology, Washington University, St. Louis, MO 63130, United States of America

ARTICLE INFO

Article history:
Received 10 March 2021
Received in revised form 11 May 2021
Accepted 2 June 2021
Available online 8 June 2021

Keywords:
Finite element analysis
Acoustic detection
Plant defenses
Herbivore identification
Structural vibration

ABSTRACT

Selective sensation of sound by the plant *Arabidopsis thaliana* may enable the timely upregulation of defensive compounds to protect against caterpillars of the plant's primary insect herbivore. Vibration of leaf trichomes has been shown to occur over frequency ranges that are appropriate for responding to these caterpillars, but the distribution of trichome shapes and sizes over a leaf means that a range of sounds could possibly be transduced. To assess how the diversity of trichomes on a leaf may affect sound transduction, we characterized the distribution of trichome sizes on a mature plant of *A. thaliana* and calculated the ensemble responses of entire leaves. Trichome sizes followed a normal distribution. Modal peaks in single trichome response spectra were at lower frequencies those of larger trichomes, roughly consistent with an inverse relationship between modal frequencies and trichome size. Ensemble response spectra for entire leaves showed frequency bands of responsiveness separated by defined band gaps, suggesting a possible mechanism for collective identification of the sounds of specific caterpillars.

1. Introduction

Many plants must compete with neighboring plants for light and resources while simultaneously deterring herbivores [1]. Winning these competitions requires the expenditure of metabolic energy, and the ability to divert this energy to the most pressing threats might offer evolutionary advantage [2,3]. For example, expenditure of energy on defensive compounds can reduce the resources available for a plant to grow sufficiently high relative to its neighbors to obtain sunlight, but insufficient energy devoted to this can leave a plant vulnerable to herbivores. This evolutionary force is believed to have given rise to mechanisms that enable plants to perceive and respond to stimuli like touch and sound [4,5].

The literature abounds with half-baked efforts to study this, with well-known early studies of the effects of music on plants now being thoroughly discredited [6]. More recent reports (*e.g.*, [7,8]) of plants responding to music suffer from limited statistical analysis and challenges with repeatability. However, a growing body of research suggests that, although plants certainly do not listen to music, they can respond to certain sound through changes to gene, protein, and hormonal expression, as well as oxygen uptake [9–14]. Studies with more believable statistics report that effects vary with the frequency of the sound waves that excite the plant, with frequencies in the 0.3–14 kHz range possibly affecting growth rates [15,16]. Certain mRNA may be elevated following excitation of 125 and 250 Hz, and decreased for excitation at 50 Hz [10]. In one of the most sophisticated and rigorous studies reporting acoustic responses by plants, Appel and Cocroft [17] report that leaves of *Arabidopsis thaliana* prime production of the insect deterrents anthocyanin and glucosinolate in response to audio recordings of the plant's primary insect herbivore, the *Pieris* caterppillar, but not in response to recordings of other caterpillars or of white noise.

Confounding the interpretation of such experiments is the lack of agreement on what parts of a plant serve as acoustic

* Corresponding authors.
E-mail addresses: tjlu@nuaa.edu.cn (T.J. Lu), sbliu@nuaa.edu.cn (S. Liu).

https://doi.org/10.1016/j.eml.2021.101377
2352-4316/

mechanosensors. Hypotheses include that of Collins [16] suggests that scrubbing of traverse waves against the leaf increase transpiration from the plant. Wang et al. [18] hypothesize that sound transduction accelerates RNA synthesis and concentrations of soluble proteins. Zhou et al. [19] note that trichomes of *A. thaliana* are mechanosensitive, with mechanostimulation leading to oscillations of Ca^{2+} and increases in pH. Liu et al. [20] found that these trichomes have vibrational modes in the frequency range of sounds of feeding caterpillars, and suggested that these trichomes may serve as acoustic antennae.

A key feature of reported responses to sound is that the responses appear to vary with frequency. Lacking in previous studies of trichome vibrations is analysis of how the many and differently sized trichomes on a leaf can collectively lead to the selective sampling of distinct frequencies. We hypothesized that trichomes contribute towards selective sound transduction in the leaves of *A. thaliana* via band gaps, a feature of modal responses whereby certain frequency ranges are transduced, while others are ignored. Although band gaps are known to appear in the acoustic responses of single trichomes [20], it is unknown whether these persist in the ensemble responses of entire leaves. To test our hypothesis, we therefore measured size distributions of trichomes on leaves of *A. thaliana*, then analyzed the modal responses of trichomes across this range of sizes.

2. Materials and methods

2.1. Quantitative microscopy of trichomes

Plants of the *Arabidopsis thaliana* ecotype Columbia were grown in a Turba substrate (Kekkila DSM 2 W) from Kekkila Garden (Vantaa, Finland) in a growth chamber with an average photon flux density of 90–120 μmol m^{-2} s^{-1} at 22 °C and a light cycle of 16 h of light (7 a.m. to 11 p.m.) and 8 h of darkness (11 p.m. to 7 a.m.). Before seeds were sown in soil, they were pretreated at 4 °C for 3 days.

For scanning electron microscopy (SEM) imaging, one-month-old *A. thaliana* leaves were freeze-dried and mounted on double-sided carbon tape, then sputtered with a thin layer of gold. To ensure uniform age and maturation of trichomes, we analyzed trichomes on the fourth leaves of a one-month-old plant. Trichomes were scanned under a focused beam of high energy electrons in a raster scan pattern using an ultrahigh resolution field emission scanning electron microscope (Merlin Compact, Carl Zeiss, Oberkochen, Germany) at 10 keV in high vacuum mode.

2.2. Discretization of trichomes

Three-dimensional solid models of trichomes were developed from microscopy images using standard computer-aided design software (Creo, PTC, Needham, MA). Dimensions of branches were taken from SEM images described above. The inner contour of the model was based on ultraviolet confocal microscopy images from the literature, and the outer contours from associated laser confocal microscopy images [19]. Based upon these data, the stalk of each trichome was axisymmetric, approximately 200 μm in height, and with a thickness profile of $t\,(x_1) = 0.0437x_1 + 3.167$ μm, where x_1 is the height along the stalk's central axis from the podium in micrometers. Three branches extended from a junction at the top of each trichome stalk, each with wall thickness $t = 1.5$ μm and an external conical boundary that tapered uniformly from the base of the branch to its sharp point.

This geometry was discretized into a mesh for finite element analysis in the Abaqus environment (Dassault Systèmes SE, Vélizy-Villacoublay, France) using three-node triangular shell elements (S3) and four-node, reduced integration quadrilateral shell elements (S4R) to mesh the cell wall of trichome.

The trichome was filled with cytoplasm with a turgor pressure, regardless of the exchange of substances between the cytoplasm and the outside of the cell. Solid–liquid coupling at the boundary between the cell plasma membrane and the cell wall was modeled using nonstructural mass elements to simulate the mass of cytoplasm, and hydrostatic fluid elements F3D3 and F3D4 to model the coupling of deformation and turgor pressure.

The cytoplasmic mass accounts for a large part of the mass of trichome cells. Due to the use of a shell model, it was necessary to consider the influence of cytoplasmic mass by attaching the cytoplasmic mass to the cell wall. However, distributing the mass of the cytoplasm evenly over the shell produces an inappropriate mass distribution that alters the mechanical properties of the model. Thus, the mass of the cytoplasm was attached to the cell wall sectionally, and the equivalent density of each part was:

$$\rho = \rho_{\text{wall}} + \frac{V_{\text{cyto}}}{V_{\text{wall}}}\rho_{\text{cyto}} \tag{1}$$

where ρ_{wall} is the density of the cell wall, ρ_{cyto} is the density of the cytoplasm, V_{cyto} is the volume of cytoplasm and V_{wall} is the volume of cell wall.

For the stalk and branches, the model was divided into several small segments, each of which was regarded as a cylinder. The volumes of cytoplasm and cell wall of each small cylinder were: $V_{\text{cyto}} = \pi(r-t)^2 h$, $V_{\text{wall}} = \pi[r^2-(r-t)^2]h$, h is the length of the cylinder, r is the radius of the cylinder. So the equivalent density of stalk and branches were: $\rho = \rho_{\text{wall}} + \frac{(r-t)^2}{2rt-t^2}\rho_{\text{cyto}}$.

The connection part between the branch and the stalk could not be considered as a collection of small cylinders. Considering it as a whole, the volume of the cytoplasm of the connected part was obtained in the solid modeling software as $V_{\text{cyto}} \approx 2.3\times10^{-14}$ m^3 and $V_{\text{cyto}} \approx 7.8 \times 10^{-15}$ m^3.

Standard FEA convergence studies were performed, with natural frequencies checked as a function of mesh size to ensure a finite element mesh sufficiently refined that further refinement would not change the first five model frequencies by more than 1%. This was achieved for finite element discretization in which the largest element had an edge length of 30 μ m; all studies used meshes with elements having edge lengths no greater than 1/10 this size.

2.3. Boundary conditions

To model the elastic and deformable leaf, the substrate was modeled as a Winkler-type foundation having an elastic stiffness k per unit area. Displacement of the foundation was limited to the horizontal plane. According to Winkler's elastic foundation theory [21], the foundation stiffness is:

$$k = \frac{E_L}{2(1-\nu_L^2)r_0} \tag{2}$$

where E_L and ν_L are the effective elastic modulus and Poisson ratio of the foundation respectively, and r_0 is the maximum radius of stalk.

2.4. Modal analysis

Modal analysis was performed using standard linear modal analysis in Abaqus 2016 (Dassault Industries, Paris, France). Via modal analysis, we estimated the natural frequencies at which trichomes may be particularly adept at transducing acoustic energy: a stimulus at a frequency close to a structure's natural frequency will cause the structure to resonate so that stimuli of small amplitude can become amplified. The natural frequency

Table 1
Mechanical properties and geometrical parameters of trichomes.

Symbol	Variable	Range	Baseline value
ρ_{wall}	Density of cell wall	Characean internode: 1.4 g/cm^3 [22] Wood: 0.1–3 g/cm^3 [23]	1 g/cm^3
ρ_{cyto}	Density of cytosol	Characean internode: 1.0 g/cm^3 [22] Pollen tube: 1 g/cm^3 [24]	1 g/cm^3
$t\,(x_1)$	Thickness of tapered stalk cell wall	1.5–6.5 μm [19]	See methods
E_{wall}	Young's modulus of cell wall	0.6–4.7 GPa [23,25]	1 GPa
E_L	Young's modulus of trichome foundation	0.035–35 GPa [23]	1 GPa
k	Foundation stiffness	Animal cells: 10^{-5}–10^{-2} MPa/μm [26] Plant cells: 1–30 MPa/μm (estimated)	10 MPa/μm
ν_L	Poisson's ratio of trichome foundation	0.30–0.49 [27]	0.33
κ_{cyto}	Bulk modulus of cytosol	2.15 GPa [28]	2.15 GPa
p_0	Turgor pressure of cell	0.8–1.4 MPa [29] Guard cells 0.5–5 MPa [30]	0.5 MPa

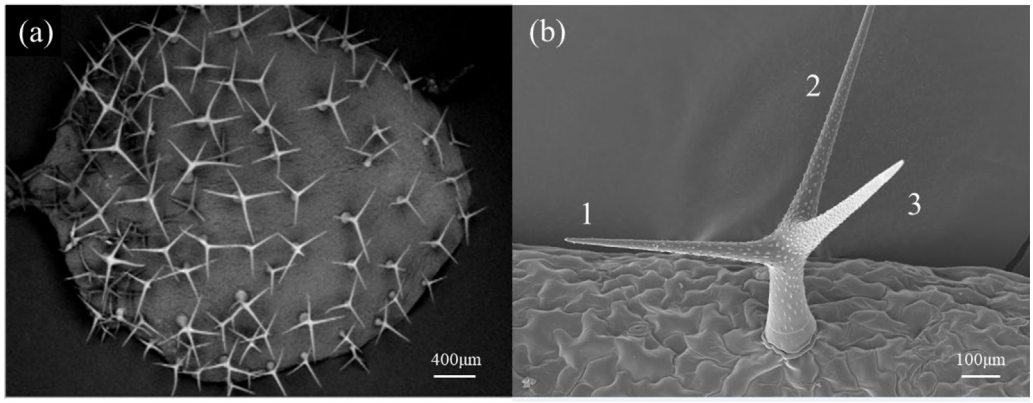

Fig. 1. Scanning electron microscopy images of trichomes on a leaf of *Arabidopsis thaliana*. (a) A population of trichomes on a leaf. (b) A single trichome.

depends upon the geometry and mechanical properties of a structure, and does not vary with time. Mathematically, natural frequencies are the eigenvalues of the equations of motion, while mode shapes correspond to the associated eigenvectors. The generalized equation of motion for a discretized trichome structure was analyzed:

$$\mathbf{M}\left[\mathrm{d}^2\mathbf{X}\,(t)\,/\mathrm{d}t^2\right]+\mathbf{K}\mathbf{X}\,(t)=0 \tag{3}$$

where $\mathbf{M}$ is a matrix of effective nodal masses, $\mathbf{X}\,(t)$ is a vector of nodal displacements, $\mathbf{K}$ is a matrix of effective stiffnesses. Baseline parameter values were as listed in Table 1. The patterns of free vibration that an acoustic wave would excite are the vectors $\mathbf{X}\,(t)$ that satisfy the homogeneous version of the differential equation with the form $\mathbf{X}\,(\mathrm{t})=\mathbf{X}_0\exp(i\omega t)$, where $i=\sqrt{-1}$, $\mathbf{X}_0$ represents mode shape, and ω represents the associated natural frequencies. Substituting these into Eq. (3) results in the well-known modal analysis eigenvalue equation that can be solved to find $\mathbf{X}_0$ and ω:

$$\left(\mathbf{K}-\omega^2\mathbf{M}\right)\mathbf{X}_0=\mathbf{0} \tag{4}$$

2.5. Spectral analysis

Finite-element analysis was performed to analyze vibration of trichome structures. The generalized equation of motion for a discretized trichome structure was analyzed:

$$\mathbf{M}\left[\mathrm{d}^2\mathbf{X}\,(t)\,/\mathrm{d}t^2\right]+\mathbf{K}\mathbf{X}\,(t)=\mathbf{F}(t) \tag{5}$$

where $\mathbf{F}\,(t)=f_0\sin\omega t$ is a vector of applied forces, and ω is angular frequency. The displacement response of points of trichome structure can be obtained through the finite-element modal analysis.

The amplitude spectrum $\hat{x}\,(\omega)$ is the Fourier transform of $x\,(t)$:

$$\hat{x}\,(\omega)=\int_{-\infty}^{\infty}x_T\,(t)\,e^{-i\omega t}\mathrm{d}t \tag{6}$$

where $x\,(t)$ is the displacement at the tip of trichome branch 1, $x_T\,(t)=\begin{cases}x\,(t)\,, & |t|<T\\ 0, & |t|>T\end{cases}$, T is the time of signal acquisition.

The energy spectral density is:

$$E_x\,(\omega)=|\hat{x}\,(\omega)\,|^2 \tag{7}$$

2.6. Scaling law

For the stalk of a trichome, the natural frequency of the lowest torsional mode [31] is approximately:

$$f_t=\frac{1}{2\pi}\sqrt{\frac{K}{I_{xx}^P}} \tag{8}$$

where $K=\frac{\pi}{4}\frac{E}{H(1+\nu)}\left[r_1^4-(r_1-t)^4\right]\sim L_c^3$ is the torsional rigidity of stalk, and $I_{xx}^P=\frac{\pi\rho}{20}[\left(3+3\cos^2\phi\right)r_0^4L+2\sin^2\phi L^3r_0^2]\sim L_c^5$ is the moment of inertia, in which L_C is the characteristic size of a trichome (*i.e.*, length of branch 1), E is the Young's modulus of cell wall, ρ is the density of the trichome, H is the length of the stalk, r_0 is the maximum radius of the stalk, and r_1 is the maximum radius of the branch. Thus we expect:

$$f_t\sim L_c^{-1} \tag{9}$$

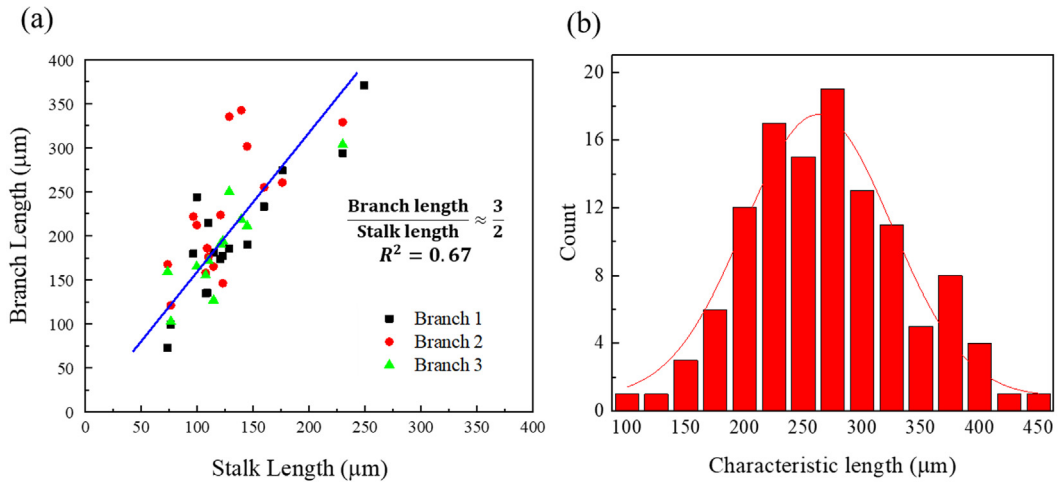

Fig. 2. The size distribution of trichomes on a leaf. (a) The length distribution of trichome branches on a leaf. The ratio of branch length to stalk length is approximately 1.5 ($R^2 = 0.67$). Because the length of branch 1 is proportional to that of other branches and stalk, we defined the length of branch 1 as the characteristic length of trichome. (b) Distribution of characteristic lengths of trichomes on a leaf approximately followed a normal distribution.

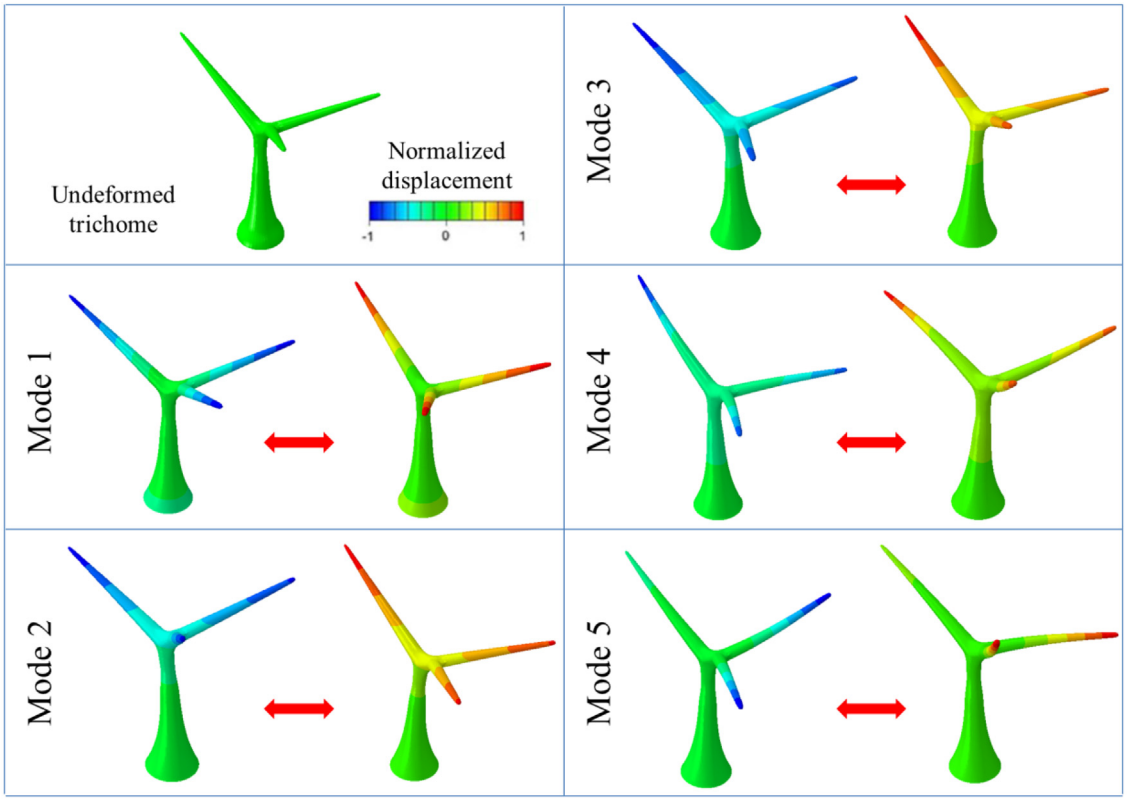

Fig. 3. The modal shapes of trichome vibration. The length of branch 1 is 263 μm. The first mode is torsional vibration of the stalk, with the branches rotating together, nearly as a rigid body. The second and third modes were different flexural vibrations of the stalk, again with the branches moving like a rigid body; the mode frequency curves for these two analogous vibrations were close. The fourth and fifth mode shapes represented flexural vibration of the branches, and the mode frequency curves were thus also close. The higher order modal shapes combined vibration of the stalk and branches. Modal shapes are better visualized through animations provided in Movies S1–S5.

For the stalk of a trichome, the natural frequency of the nth order flexural mode is:

$$f_n = \frac{\pi}{2}\left(\frac{n}{H}\right)^2\sqrt{\frac{EI}{\rho A}} \sim L_c^{-1} \tag{10}$$

where $I = \frac{\pi r_1^4}{64} \sim L_c^4$ is the second moment of the cross-sectional area and $A = \pi r_1^2 \sim L_c^2$ is the basal area of stalk.

For a branch of a trichome, based on the theory of a conical beam, the natural frequency of the nth order flexural mode [32] is:

$$f_n = \frac{1}{4\pi}\beta_n \frac{r_0}{L^2}\sqrt{\frac{E}{\rho}} \sim L_c^{-1} \tag{11}$$

where $\beta_n = \{8.72, 21.2, 38.5, 60.7\cdots\}$. This scaling is analogous to that of a classical mass-spring system, for which $f \propto$

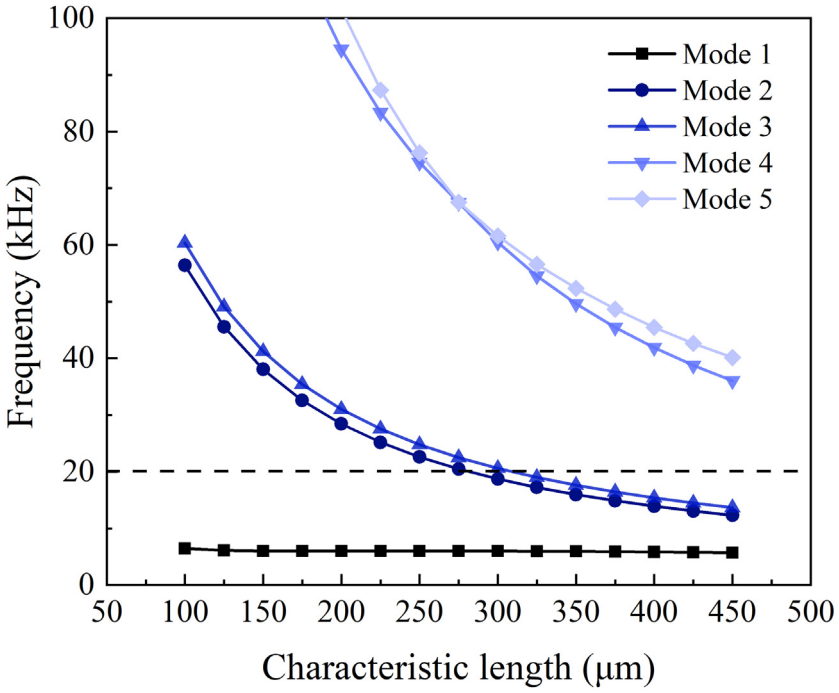

Fig. 4. Relationship between natural frequencies of trichomes and their characteristic lengths. The ∼6 kHz natural frequency of first mode changes little with trichome size and shows a band gap with other modes. The natural frequencies of higher modes decrease with increasing trichomes size. The natural frequencies of second and third modes are close and range ∼10–60 kHz. The natural frequencies of fourth and fifth modes are close and much larger.

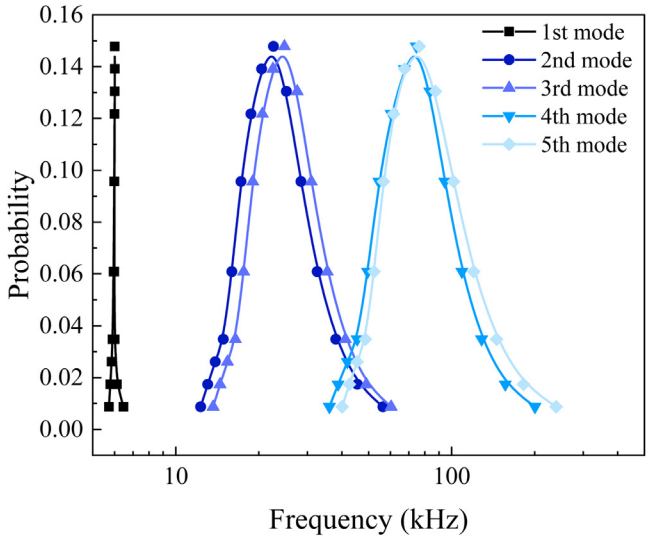

Fig. 5. Probability distribution of the natural frequencies for the first five modes. The probability distribution of the first–fifth modes can be seen as normal distribution with the following expectation and standard deviation: $f_1 = 6.02 \pm 0.05$ kHz; $f_2 = 23.3 \pm 5.09$ kHz; $f_3 = 25.5 \pm 5.47$ kHz; $f_4 = 76.4 \pm 18.5$ kHz; $f_5 = 80.6 \pm 19.2$ kHz.

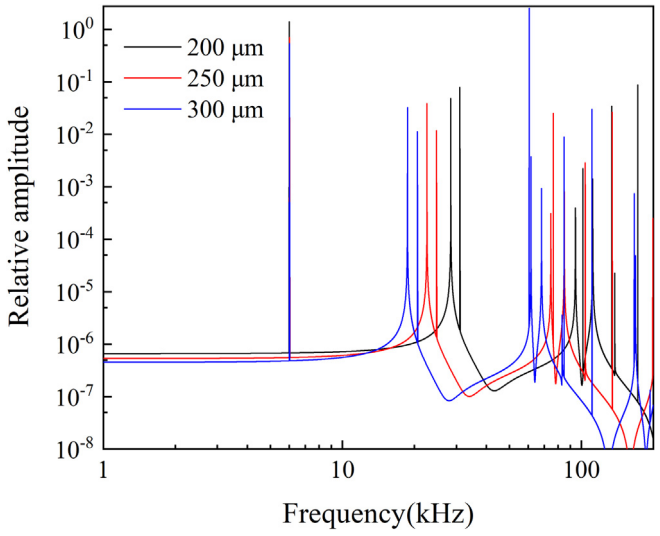

Fig. 6. Amplitude spectra of trichomes with different sizes. The spike of relative amplitude for the first mode is concentered and separate from other spikes, while the spikes of relative amplitude for the second and third modes are close. With the increasing trichome size, spikes shift to lower frequencies.

$\sqrt{k/m}$, where k is the spring stiffness and m is the mass. For a self-similar structure, $k \propto L$ and $m \propto L^3$, so that $f \sim L^{-1}$.

3. Results

SEM images of *A. thaliana* leaves (Fig. 1) revealed that the sizes of trichomes approximately followed a normal distribution, with branch lengths of 263 ± 62.7 μm (mean ± standard deviation, Fig. 2(a)), and a mean ratio of branch length to stalk length of approximately 1.5 (Fig. 2(b)).

The natural frequencies and modes are the eigenvalues and eigenvectors of the structure, and reflect the dynamical properties of the structure of a trichome. We performed modal analysis (Fig. 3) and calculated how natural frequencies of trichomes vary with trichome size (Fig. 4).

The first five modes represented torsion and flexure of the stalk and branches (Fig. 3). The first order mode shape was torsional vibration of stalk with the three branches rotating about the axis as a rigid body. The second and third order mode shapes represented flexural vibration of the stalk, again with the branches mostly moving as a single rigid body. Higher

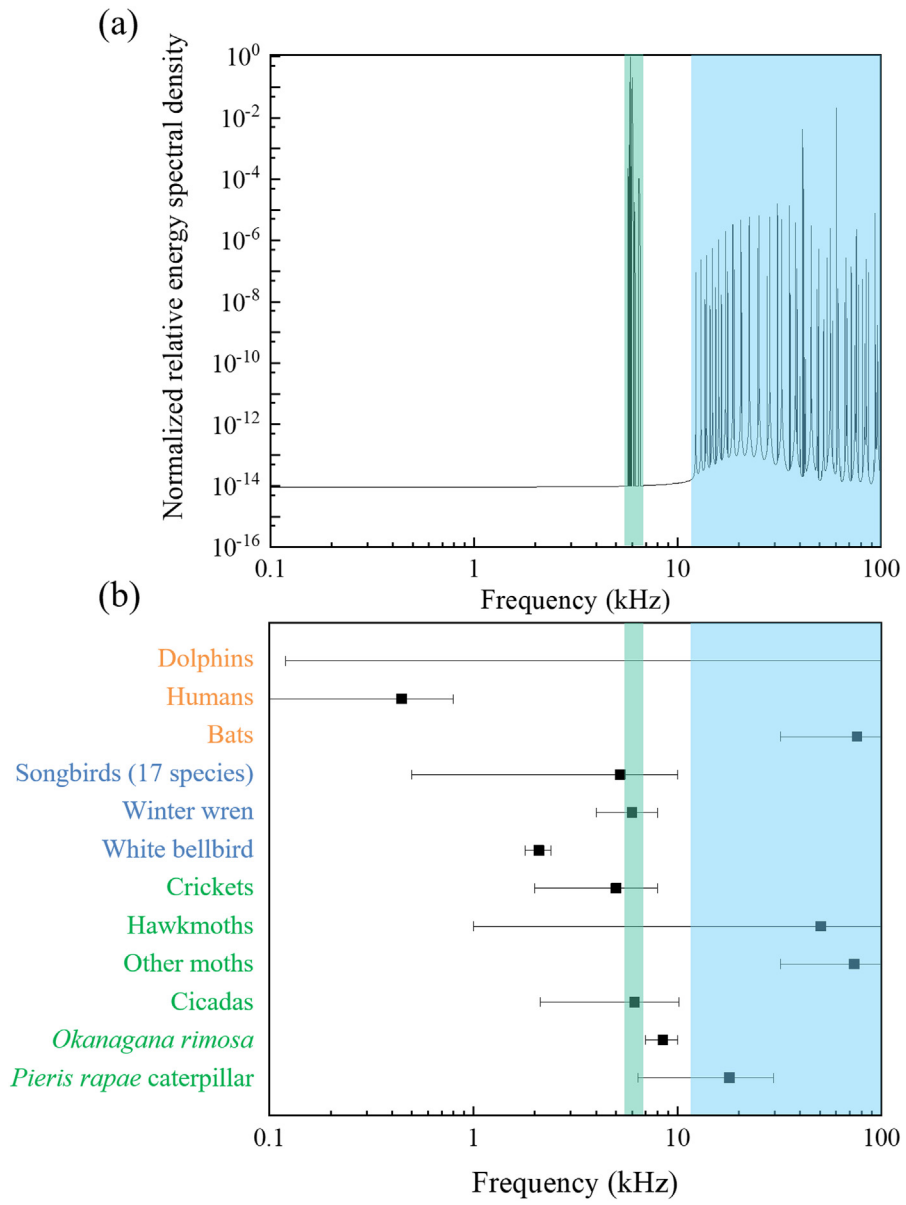

Fig. 7. (a) Energy spectrum of trichomes on an *Arabidopsis* leaf. (b) Range of sound frequency emissions for a range for different species. A band gap exists between the 5.7–6.2 kHz spikes and the band of reception above 12 kHz. The caterpillar of *Pieris rapae* is unusual in that it is one of only a handful of land-based animals active during the day that produces acoustic emissions over both ranges of potential signal transduction by *A. thaliana*.

order modal shapes were a composite of vibrations of stalks and branches.

The lowest resonant frequencies of trichomes across the range of sizes was on the order of 6 kHz, and varied little with respect to the size of the trichome (Fig. 4). The natural frequencies of the second to fifth order modes were around 12–58 kHz, 13–61 kHz, 36–200 and 40–240 kHz. From second to fifth order modes, the natural frequencies decreased with the increasing size of trichomes. The natural frequencies of the second and third modes were very close, as were those of the fourth and fifth modes.

The ensemble response of trichomes on a leaf was estimated by combining size-specific modal responses according to the probability distribution of trichome sizes across the first five modes. The resulting probability distribution of natural frequencies (Fig. 5) reveals a composite response with three bands and two distinct band gaps in the 0–200 kHz range. These follow an approximately normal distribution with the following means and standard deviation: $f_1 = 6.02 \pm 0.05$ kHz; $f_2 = 23.3 \pm 5.09$ kHz; $f_3 = 25.5 \pm 5.47$ kHz; $f_4 = 76.4 \pm 18.5$ kHz; $f_5 = 80.6 \pm 19.2$ kHz. The second and third modes overlapped extensively, as did the fourth and fifth modes.

We performed harmonic response analysis [33] to predict the steady-state responses of individual trichomes under harmonic loading. Trichomes of different sizes each showed response spectrum of different relative amplitude (Fig. 6). The first spike of relative amplitude was, in all cases, concentered at ∼6 kHz and separate from other spikes, while the spikes of relative amplitude for the second and third modes were close, as were spikes associated with the fourth and fifth modes. With increasing of trichome size, spikes shifted to lower frequencies. The peaks of the amplitude spectrum corresponded to the natural frequencies of trichome vibration.

Although amplitude spectra cannot be superimposed, energy spectra are scalar quantities and thus superposable. The energy spectral density of trichomes of different sizes was calculated via

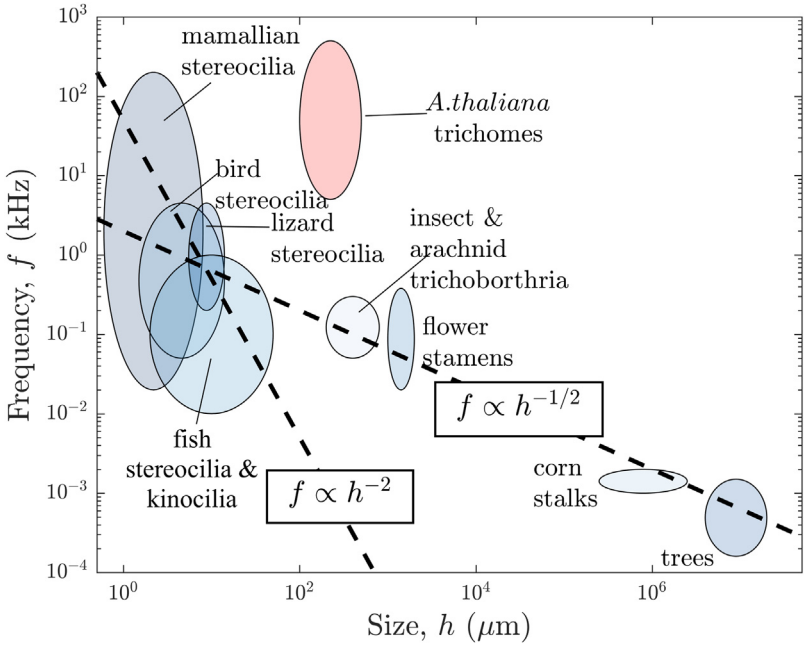

Fig. 8. Audible frequency *versus* the size of hair cells. Data are listed in Table 2. The torsional responses of the trichomes of *A. thaliana* enable frequency transduction over a range that lies far outside of the range of similarly sized acoustic receptors from other species.

Eq. (7), and weighted summation energy spectral densities was performed following the size probability distribution. The result, for a leaf with a finite number of leaves, presented an envelope spikes of relative amplitude ranges of 5.72–6.20 kHz, and another of relative amplitude ranges above 12 kHz (Fig. 7).

4. Discussion

The ensemble response of a trichome leaf showed peaks and band gaps, supporting our hypothesis. Both individual trichomes and entire leaves had band gaps in their responses. The second and third mode frequency curves were close (Fig. 4), as expected because these two modal shapes represent flexural vibration of the stalk in two orthogonal directions (Fig. 3). For frequencies lower than 12 kHz, the relative energy spectral density has spikes near 6 kHz (Fig. 7), because the probability distribution of the first mode is concentrated at frequencies 6 kHz (Fig. 5) and the relative amplitude spectrum spikes around 6 kHz (Fig. 6).

Similarly, the fourth and fifth mode frequency curves were close (Fig. 4) as these two mode shapes represent flexural vibration of the branches (Fig. 3). The band gaps were such that resonance was expected in the 10–20 kHz range, a range over which higher frequency mechanoreception has been reported in other plants [14]. For frequencies larger than 12 kHz, the relative energy spectrum contains dense spikes (Fig. 7a), perhaps enabling further delineation of specific frequency content.

To gain confidence in the finite element methods, we examined the predictions in the context of data from the literature. The first vibrational mode, in the vicinity of 6 kHz (Fig. 4), was well within the audible range (∼20–20,000 Hz), and well within the range for which Pieris feeding noises present substantial power (below ∼8 kHz, [20]). The 6 kHz range is on the order of primary frequencies reported for mechanotransduction in several other plants as well [15,16]. As is evident from Fig. 4, the natural frequencies of the higher modes were very sensitive to trichome size over the range of smaller characteristic trichome lengths, and were inversely proportional to the size of trichomes (Fig. 4), consistent with the scaling laws we derived (*i.e.*, Eqs. (10) and (11)).

Comparison of these spectra to the relative emission spectrum of a *Pieris* caterpillar chewing the leaf of its primary food [17], a leaf of *A. thaliana*, suggests that, if acoustic reception by trichomes is indeed the means of acoustic signal transduction, the 6 kHz peak would be a likely trigger, because this is the region of strong overlap between the two spectra (Fig. 7). This peak is the only natural frequency strongly conserved across all trichomes, and could therefore serve as a relatively robust mechanosensor. However, because white noise and a range of animals can also excite this natural resonant frequency (Fig. 7b), additional information must be transduced to explain the sound specificity observed by Appel and Cocroft: the specificity of defensive compound priming to activation by the sounds of *Pieris* caterpillars requires more than a single peak of acoustic excitation. Because differently sized trichomes combine to endow a leaf with relatively uniform frequency response at higher frequencies, high frequency signal transduction appears unlikely. One possibility is that periodicity of 6 kHz excitation associated with periodic chewing by *Pieris* caterpillars, combined with the refractory interval of the ion channels that become activated, may combine to enable acoustic signal specificity. Another intriguing possibility is that *A. thaliana* draws responses from the two separate bands of trichome vibration, harnessing an unusual feature of the caterpillar or *Pieris rapae* to distinguish it from other animals: as is evident from Fig. 7b, this caterpillar, the primary insect herbivore of *A. thaliana*, is unusual amongst land-based animals active during the day in that produces acoustic emissions over both ranges of potential signal transduction by *A. thaliana*.

Comparing trichomes of *A. thaliana* to other acoustic receptors in the natural world is an interesting exercise. Animal hair cells sense sound waves through acoustically driven stretch-activated ion channels [55,56], resulting in ranges of audible frequencies similar to those of trichomes, but with much smaller receptors (Table 2). As with trichomes, the frequencies audible by animals are inversely proportionally to the geometrical sizes of stereocilia (Fig. 8).

Data from the literature follow two separate trendlines (Fig. 8). For sterocilia, the range of hearing as a function of hair size follows the scaling law for the frequency response of a cantilever

Table 2
Natural frequency and size of different species.

Species	Size	Audible frequency
Trichome	75–370 μm (branch of *Arabidopsis* trichome) 70–250 μm (stalk of *Arabidopsis* trichome) 285, 382 μm (branch of *Arabidopsis* trichome, measured from figure) [34] 175 μm (stalk of *Arabidopsis* trichome, measured from figure) [34]	∼kHz (*Arabidopsis*) [17,20]
Mammals	1.2–5.8 μm (stereocilia, Guinea pigs, measured from figure) [35] 0.6–5.8 μm (stereocilia, chinchilla, measured from figure) [35] 2.3–4.3 μm (stereocilia, rat) [37] 2.5–7 μm (stereocilia, bat) [37] 2.5–8 μm (stereocilia, human, measured from figure) [35]	0.045–49 kHz (guinea pigs, 60 dB SPL) [36] 0.05–33 kHz (chinchilla, 60 dB SPL) [36] 0.1–12.6 kHz (mole rat) [38] 23–111 kHz (bat *Pteronotus*) [39] 13–73 kHz (bat *Tadarida*, measured from figure) [40] 0.02–20 kHz (human) [41]
Lizards	5.5–14 μm (stereocilia, bobtail lizard *Tiliqua rugosa*) [42]	0.2–4.5 kHz (bobtail lizard *Tiliqua rugosa*) [43]
Birds	3–10 μm (stereocilia, emu) [44] 1.5–5.3 μm (stereocilia, chicken) [46]	0.05–3.3 kHz (emu) [45] 0.07–3.3 kHz (chicken) [47]
Fish	2–50 μm (stereocilia) [48]	0.01–1 kHz [48]
Arthropod	200–800 μm (trichobothria, spider) [49]	0.05–0.3 kHz (spider) [49]
Tree	4–20 m (lime tree) [50] 12–18 m (red maple) [51] 6–19 m (spruce) [52] 7.9–18.5 m (pine) [52] 14.3–20 m (Douglas fir) [52]	0.3–1.5 Hz (lime tree) [50] 0.2–0.3 Hz (red maple) [51] 0.25–1.39 Hz (spruce) [52] 0.16–0.6 Hz (pine) [52] 0.3–0.66 kHz (Douglas fir) [52]
Corn	0.25–2.5 m [53]	1–2 Hz [53]
Flower	1000–2000 μm (Stamen) [54]	0.02–0.38 kHz [54]

beam, with $f \propto h^{-2}$. This is expected because the vibration mode of stereocilia is typically flexural, as in modes 2-3 for *Arabidopsis* trichomes. For larger hairs, plants, and plant structures, the data follow a weaker scaling, with $f \propto h^{-1/2}$. The ellipse representing *A. thaliana* trichomes deviates substantially from those of other species, indicating that *Arabidopsis* trichomes have adapted to enable resonance at relatively high frequencies despite their large size. The key to these adaptations can be understood from the trichome mode shapes (Fig. 3): the branched structure of the trichomes enables torsional modes of vibration that permit both the high- and low-band frequency transduction shown in Fig. 7. The torsional responses of the trichomes of *A. thaliana* thereby enable frequency transduction over a range that lies far outside of the range of similarly sized acoustic receptors from other species.

5. Conclusion

Both individual trichome and ensembles of trichomes on a leaf of *A. thaliana* show resonance in the range of acoustic emissions by the *Pieris* caterpillar. Resonant frequencies are inversely proportional to the sizes of trichomes, with peaks of amplitude spectra shifting to lower frequencies with increasing trichome size. The energy spectrum spikes for individual trichomes on a leaf are intermittent, but the first mode of vibration has a resonant frequency that is highly conserved across trichome sizes and that is separated from all other modes by a band gap, even when combined with trichomes of the observed normally distributed sizes and on a very large leaf. The fact that acoustic emissions of the Pieris caterpillar crosses both of these bands of reception may help with selective transduction of these emissions by *Arabidopsis*. These data identify target frequency ranges for future experimentation on acoustic reception by trichomes that seek to verify acoustically-driven mechanosensing.

Declaration of competing interest

The authors declare that they have no known competing financial interests or personal relationships that could have appeared to influence the work reported in this paper.

Acknowledgments

This work was supported by the National Natural Science Foundation of China (11902155, 12032010 and 11902245), by the Natural Science Foundation of Jiangsu Province (BK20190382), by the foundation of Jiangsu Provincial Key Laboratory of Bionic Functional Materials, by the Foundation for the Priority Academic Program Development of Jiangsu Higher Education Institutions, by the National Science Foundation through the Science and Technology Center for Engineering Mechanobiology (CMMI 1548571).

Appendix A. Supplementary data

Supplementary material related to this article can be found online at https://doi.org/10.1016/j.eml.2021.101377.

References

[1] F. Takahashi, K. Shinozaki, Long-distance signaling in plant stress response, Curr. Opin. Plant Biol. 47 (2019) 106–111.
[2] C. Dobrota, Energy dependant plant stress acclimation, Rev. Environ. Sci. Biol. 5 (2–3) (2006) 243–251.
[3] R.C. Mishra, R. Ghosh, H. Bae, Plant acoustics: in the search of a sound mechanism for sound signaling in plants, J. Exp. Bot. 67 (15) (2016) 4483–4494.
[4] E.W. Chehab, E. Eich, J. Braam, Thigmomorphogenesis: a complex plant response to mechano-stimulation, J. Exp. Bot. 60 (1) (2008) 43–56.
[5] T. Hou, B. Li, G. Teng, L. Qi, K. Hou, Research and application progress of plant acoustic frequency technology, J. China Agric. Univ. 15 (1) (2010) 106–110.
[6] R.M. Klein, P.C. Edsall, On the reported effects of sound on the growth of plants, Bioscience 15 (2) (1965) 125–126.
[7] V. Chivukula, S. Ramaswamy, Effect of different types of music on Rosa chinensis plants, Int. J. Environ. Sci. Dev. 5 (5) (2014) 431.
[8] D. Sharma, U. Gupta, A.J. Fernandes, H.A. Solanki, The effect of music on physico-chemical parameters of selected plants, Int. J. Plant Anim. Environ. Sci. 5 (1) (2015) 282–287.
[9] R.H. Hassanien, T. Hou, Y. Li, B. Li, Advances in effects of sound waves on plants, J. Integr. Agric. 13 (2) (2014) 335–348.
[10] M.J. Jeong, C.K. Shim, J.O. Lee, H.B. Kwon, Y.H. Kim, S.K. Lee, M.O. Byun, S.C. Park, Plant gene responses to frequency-specific sound signals, Mol. Breeding 21 (2) (2008) 217–226.
[11] R. Ghosh, M.A. Gururani, L.N. Ponpandian, R.C. Mishra, S.C. Park, M.J. Jeong, H. Bae, Expression analysis of sound vibration-regulated genes by touch treatment in arabidopsis, Front. Plant Sci. 8 (100) (2017) 334–339.

[12] B. Choi, R. Ghosh, M.A. Gururani, G. Shanmugam, J. Jeon, J. Kim, S.C. Park, M.J. Jeong, K.H. Han, D.W. Bae, H. Bae, Positive regulatory role of sound vibration treatment in *arabidopsis thaliana* against botrytis cinerea infection, Sci. Rep. 7 (1) (2017) 2527.
[13] M.G. Schöner, R. Simon, C.R. Schöner, Acoustic communication in plant–animal interactions, Curr. Opin. Plant Biol. 32 (2016) 88–95.
[14] Y.C. Qin, W.C. Lee, Y.C. Choi, T.W. Kim, Biochemical and physiological changes in plants as a result of different sonic exposures, Ultrasonics 41 (5) (2003) 407–411.
[15] P. Weinberger, M. Measures, Effects of the intensity of audible sound on the growth and development of rideau winter wheat, Can. J. Bot. 57 (9) (1979) 1036–1039.
[16] M.E. Collins, J.E. Foreman, The effect of sound on the growth of plants, Can. Acoust. 29 (2) (2001) 3–8.
[17] H.M. Appel, R. Cocroft, Plants respond to leaf vibrations caused by insect herbivore chewing, Oecologia 175 (4) (2014) 1257–1266.
[18] X. Wang, B. Wang, Y. Jia, C. Duan, A. Sakanishi, Effect of sound wave on the synthesis of nucleic acid and protein in chrysanthemum, Colloid Surf. B 29 (2–3) (2003) 99–102.
[19] L.H. Zhou, S.B. Liu, P.F. Wang, T.J. Lu, F. Xu, G.M. Genin, B.G. Pickard, The *arabidopsis* trichome is an active mechanosensory switch, Plant Cell Environ. 40 (5) (2017) 611–621.
[20] S. Liu, J. Jiao, T.J. Lu, F. Xu, B.G. Pickard, G.M. Genin, Arabidopsis leaf trichomes as acoustic antennae, Biophys. J. 113 (9) (2017) 2068–2076.
[21] V.A. Lubarda, Circular loads on the surface of a half-space: displacement and stress discontinuities under the load, Int. J. Solids Struct. 50 (1) (2013) 1–14.
[22] R. Wayne, M.P. Staves, J. Plant, C. Physiology, The density of the cell sap and endoplasm of nitellopsis and chara, Plant Cell Physiol. 32 (8) (1991) 1137.
[23] L.J. Gibson, The hierarchical structure and mechanics of plant materials, J. R. Soc. Interface 9 (76) (2012) 2749–2766.
[24] J.H. Kroeger, F.B. Daher, M. Grant, A.J. Geitmann, Microfilament orientation constrains vesicle flow and spatial distribution in growing pollen tubes, Biophys. J. 97 (7) (2009) 1822–1831.
[25] M. Probine, R.J. Preston, Cell growth and the structure and mechanical properties of the wall in internodal cells of nitella opaca: II. Mechanical properties of the walls, J. Exp. Bot. 13 (1) (1962) 111–127.
[26] V.S. Deshpande, R.M. McMeeking, A.G. Evans, A bio-chemo-mechanical model for cell contractility, P. Natl. Acad. Sci. 103 (38) (2006) 14015–14020.
[27] E. Chanliaud, K.M. Burrows, G. Jeronimidis, M.J. Gidley, Mechanical properties of primary plant cell wall analogues, Planta 215 (6) (2002) 989–996.
[28] Y. Liu, S. Thomopoulos, C. Chen, V. Birman, M.J. Buehler, G.M. Genin, Modelling the mechanics of partially mineralized collagen fibrils, fibres and tissue, J. R. Soc. Interface 11 (92) (2014) 20130835.
[29] E. Forouzesh, A. Goel, S.A. Mackenzie, J.A. Turner, In vivo extraction of arabidopsis cell turgor pressure using nanoindentation in conjunction with finite element modeling, Plant J. 73 (3) (2013) 509–520.
[30] P.J. Franks, T.N. Buckley, J.C. Shope, K.A. Mott, Guard cell volume and pressure measured concurrently by confocal microscopy and the cell pressure probe, Plant Physiol. 125 (4) (2001) 1577–1584.
[31] J. Ginsberg, W. Seemann, Mechanical and structural vibrations: theory and applications, Appl. Mech. Rev. 54 (4) (2001).
[32] D. Wrinch, On the lateral vibrations of bars of conical type, P. R. Soc. Lond. A. 101 (713) (1922) 493–508.
[33] C. Ramesha, K. Abhijith, A. Singh, A. Raj, C.S. Naik, Modal analysis and harmonic response analysis of a crankshaft, Int. J. Emerg. Technol. Adv. Eng. (2015) 2250–2459.
[34] G. Brininstool, R. Kasili, L.A. Simmons, V. Kirik, M. Hülskamp, J.C. Larkin, Constitutive expressor of pathogenesis-related genes5 affects cell wall biogenesis and trichome development, BMC Plant Biol. 8 (1) (2008) 58.
[35] A.J. Wright, Dimensions of the cochlear stereocilia in man and the guinea pig, Hear. Res. 13 (1) (1984) 89–98.
[36] C.D. West, The relationship of the spiral turns of the cochlea and the length of the basilar membrane to the range of audible frequencies in ground dwelling mammals, J. Acoust. Soc. Am. 77 (3) (1985) 1091–1101.
[37] R.R. Fay, Comparative Hearing: Mammals, Vol. 4, Springer Science & Business Media, 2012.
[38] M. Müller, B. Laube, H. Burda, V. Bruns, Structure and function of the cochlea in the african mole rat (cryptomys hottentotus): evidence for a low frequency acoustic fovea, J. Comp. Physiol. A 171 (4) (1992) 469–476.
[39] M. Kössl, M. Vater, The cochlear frequency map of the mustache bat, pteronotus parnellii, J. Comp. Physiol. A 157 (5) (1985) 687–697.
[40] M. Vater, W. Siefer, The cochlea of tadarida brasiliensis: specialized functional organization in a generalized bat, Hear. Res. 91 (1–2) (1995) 178–195.
[41] D. Manoussaki, E.K. Dimitriadis, R.S. Chadwick, Cochlea's graded curvature effect on low frequency waves, Phys. Rev. Lett. 96 (8) (2006) 088701.
[42] G.A. Manley, H. Fastl, M. Kössl, H. Oeckinhhaus, G. Klump, Auditory Worlds: Sensory Analysis and Perception in Animals and Man, Wiley Online Library, 2000.
[43] G.A. Manley, C. Köppl, B.M. Johnstone, Peripheral auditory processing in the bobtail lizard *tiliqua rugosa*, J. Comp. Physiol. A 167 (1) (1990) 89–99.
[44] F.P. Fischer, Hair cell morphology and innervation in the basilar papilla of the emu (dromaius novaehollandiae), Hear. Res. 121 (1–2) (1998) 112–124.
[45] C. KöPpl, G.A. Manley, Frequency representation in the emu basilar papilla, J. Acoust. Soc. Am. 101 (3) (1997) 1574–1584.
[46] L.G. Tilney, J.C. Saunders, Actin. filaments, stereocilia, Actin filaments stereocilia and hair cells of the bird cochlea. I. Length, number, width, and distribution of stereocilia of each hair cell are related to the position of the hair cell on the cochlea, J. Cell Biol. 96 (3) (1983) 807–821.
[47] G.A. Manley, A. Kaiser, J. Brix, O. Gleich, Activity patterns of primary auditory-nerve fibres in chickens: Development of fundamental properties, Hear. Res. 57 (1) (1991) 1–15.
[48] R.R. Fay, Comparative Hearing: Fish and Amphibians, Vol. 11, Springer Science & Business Media, 1998.
[49] F.G. Barth, A.J. Höller, Dynamics of arthropod filiform hairs. V, Response Spider Trichobothria Natl. Stimuli 354 (1380) (1999) 183–192.
[50] C.J. Baker, Measurements of the natural frequencies of trees, J. Exp. Bot. 48 (5) (1997) 1125–1132.
[51] M. Dargahi, T. Newson, J.J. Moore, A numerical approach to estimate natural frequency of trees with variable properties, Forests 11 (9) (2020) 915.
[52] J.R. Moore, D.A.J.T. Maguire, Natural sway frequencies and damping ratios of trees: concepts, review and synthesis of previous studies, Trees 18 (2) (2004) 195–203.
[53] T. Flesch, R.J. Grant, The translation of turbulent wind energy to individual corn plant motion during senescense, Bound-Lay. Meteorol. 55 (1) (1991) 161–176.
[54] C.E. Nunes, L. Nevard, F. Montealegre-Zapata, M.J. Vallejo-Marin, Are flowers tuned to buzzing pollinators? Variation in the natural frequency of stamens with different morphologies and its relationship to bee vibrations, 2020, bioRxiv.
[55] A. Vavakou, N.P. Cooper, M. van der Heijden, The frequency limit of outer hair cell motility measured in vivo, Elife 8 (2019) e47667.
[56] F. Mammano, J.F. Ashmore, Reverse transduction measured in the isolated cochlea by laser michelson interferometry, Nature 365 (6449) (1993) 838–841.